



# Influence of incorporation of Na on *p*-type CuInS<sub>2</sub> thin films

Tetsuya Yamamoto<sup>a,\*</sup>, Koichi Fukuzaki<sup>b</sup>, Shigemi Kohiki<sup>b</sup>

<sup>a</sup> Department of Electronic and Photonic Systems Engineering, Kochi University of Technology, Japan

<sup>b</sup> Department of Materials Science, Faculty of Engineering, Kyusyu Institute of Technology, Japan

## Abstract

We have investigated the electronic structures of Na-incorporated In-rich CuInS<sub>2</sub> based on ab initio electronic band structure calculations and X-ray photoelectron spectroscopy (XPS). From the results of theoretical calculations and experiments, for *p*-type In-rich CuInS<sub>2</sub> films, we find that interstitial Na species, except for Na at Cu sites, are very unstable and move easily within the crystal. This indicates that the mobile Na will act as a passivator of donor states, such as In at Cu sites and interstitial In, leading to good *p*-type conductivity of CuInS<sub>2</sub> films. On the other hand, we conclude that the formation of the ionic chemical bonds of Na at Cu sites - S atoms near the surface are energetically favorable due to a decrease in the Madelung energy. This results in the stabilization of ionic charge distributions of CuInS<sub>2</sub>:Na<sub>Cu</sub> with a shift in the energy levels of S 3*p* orbitals in the vicinity of the Na atoms towards lower energy regions. As a result, the Na incorporation yielded a surface layer of expressed as (Na,Cu) InS<sub>2</sub> on *p*-type In-rich CuInS<sub>2</sub> thin films. © 2000 Elsevier Science B.V. All rights reserved.

PACS: 73.20.At

Keywords: CuInS<sub>2</sub> thin films; Na; *p*-type; Electronic structure; Solar cell

## 1. Introduction

Chalcopyrite structure CuInS<sub>2</sub> thin films are being extensively considered for use in high-efficiency photovoltaic cells due to their direct band-gap energy being close to the required value for achieving the optimum efficiency of solar photovoltaic conversion (approximately 1.5 eV) and a large absorption coefficient for solar radiation.

Recently, the sodium effect [1,2] has become one of the important factors raising up largely the energy

conversion efficiency of solar cells using *n*-CdS/*p*-CuInS<sub>2</sub>, as well as *n*-CdS/*p*-Cu(In,Ga)Se<sub>2</sub> [3–6], thin films as absorption layers. Enhancements in conductivity, crystallite quality and device performance in controlled Na-incorporated Cu-poor CuInS<sub>2</sub> (CuInS<sub>2</sub>:Na) have been reported [1,2]. To date, the energy conversion efficiency of over 12% was achieved with a ZnO/*n*-CdS/*p*-CuInS<sub>2</sub>/Mo cell structure using only Cu-rich CuInS<sub>2</sub> films. For the Cu-rich CuInS<sub>2</sub> films, it is well known that a Cu binary phase formed at the surface of the films promotes the formation of large grains. As a result, the conductivity of 10<sup>-2</sup> S cm<sup>-1</sup> [7] of *p*-type Cu-rich CuInS<sub>2</sub> films is considerably higher than that of Cu-poor CuInS<sub>2</sub> films. On the other hand, very low conductivity of *p*-type Cu-poor CuInS<sub>2</sub> films can be due to high concentration of donor

\* Corresponding author. 185 Miyanokuchi, Tosayamada-cho, Kami-gun, Kochi 782-8502, Japan. Tel.: +81-887-57-2112; fax: +81-887-57-2120.

E-mail address: yamateko@ele.kochi-tech.ac.jp (T. Yamamoto).

states originated in intrinsic defects, such as In at Cu sites ( $\text{In}_{\text{Cu}}$ ) and S vacancies ( $\text{V}_{\text{S}}$ ). Scheer et al. precisely controlled the cooling rate in order to reduce the number of donor states, succeeding in enhancing the conductivity of Cu-poor  $\text{CuInS}_2$  films. They proposed a model showing that the enhancement was mainly due to the saturation of donor states [8].

Very recently, we have carried out the electronic-band-structure calculations [9] and systematic X-ray photoelectron spectroscopy (XPS) [10] for Cu-poor  $\text{CuInS}_2$  films incorporated with Na species ( $\text{CuInS}_2:\text{Na}$ ). Preparation of the Na-incorporated  $\text{CuInS}_2$  films used in the experiments are described elsewhere in detail [1,2]. The XPS study of  $\text{CuInS}_2:\text{Na}$  has revealed that intragrain Na species are present near the surface and chemically bonded to S atoms [10]. On the other hand, Watanabe et al. [11] measured the conductivity and photoluminescence of Cu-poor  $\text{CuInS}_2:\text{Na}$  films. They concluded that the enhancement in the conductivity of the films above was attributed to the annihilation of donor states.

The objective of this paper is to provide answers in detail, based on the results of *ab initio* electronic band structure calculations, to some questions related to the incorporation of Na: (1) How is Na incorporated into *p*-type  $\text{CuInS}_2$  thin films? Do Na species substitute Cu? Are interstitial Na species ( $\text{Na}_i$ ) stable or unstable? Moreover, does the stability of  $\text{Na}_i$  depend on the ratio of Cu to In atoms? (2) What role does Na incorporation play in the improvement of the crystallinity of *p*-type  $\text{CuInS}_2$  thin films from the view point of the formation of intrinsic and extrinsic defects, such as O species?

## 2. Methodology

In this work, we focus on Cu vacancies as the dominant intrinsic defects for *p*-type Cu-poor  $\text{CuInS}_2$  films. The reason is that the antibonding states between Cu  $3d$  ( $d\varepsilon$ ) and S  $3p$  orbitals of stoichiometric  $\text{CuInS}_2$  are located not in the conduction band but near the top of the valence band, resulting in weak Cu–S bonds [12,13].

The results of our band structure calculations for  $\text{CuInS}_2$  doped with Na or  $\text{V}_{\text{Cu}}$  are based on the local-density treatment of electronic exchange and

correlation [14–16] and on the augmented-spherical-wave (ASW) [17] formalism. The Brillouin-zone integration was carried out for 14-*k* points in an irreducible wedge. The Madelung energy, which reflects the long-range electrostatic interactions in the system, was assumed to be restricted to a sum over monopoles. For valence electrons, we employed  $3d$ ,  $4s$  and  $4p$  orbitals for Cu atoms and the outermost *s* and *p* orbitals for the other atoms. The following atomic radii (units: a.u. or atomic units) were used: 2.83 for S, 2.47 for Cu, 1.91 for In and 1.91 for Na atoms in supercells of  $\text{CuInS}_2$ , as mentioned below.

We studied the crystal structure of doped  $\text{CuInS}_2$  under periodic boundary conditions by generating supercells having 128 atoms, including 64 pseudoatoms with atomic number  $Z = 0$ , that contain the object of interest: (1) for  $\text{CuInS}_2:\text{V}_{\text{Cu}}$ , we replace one of the 16 sites of Cu atoms by a vacancy site in model supercells; (2) for  $\text{CuInS}_2:2\text{V}_{\text{Cu}}$ , we replace two of the 16 sites of Cu atoms by two vacancy sites in model supercells; (3) for Na-doped  $\text{CuInS}_2:\text{V}_{\text{Cu}}$ , we replace one of the above two Cu-vacancy sites by the Na atom site; (4) for  $\text{CuInS}_2:2\text{Na}$ , we replace two of the two Cu-vacancy sites by the two Na atom sites; (5) for  $\text{CuInS}_2:(\text{Na}_i \text{ and } \text{V}_{\text{Cu}})$ , we replace the above  $\text{Na}_{\text{Cu}}$  site of the Cu atoms by a vacancy site and one of the interstitial sites in the vicinity of the above vacancy site by the Na site. Further details are given below (see Fig. 3(a) and (b)). In this work, the effects of relaxation due to defects, such as Cu vacancies,  $\text{Na}_{\text{Cu}}$  and  $\text{Na}_i$  on the lattice constants and displacement of atoms in the vicinity of the defects, are neglected because the magnitude of change in the total energy due to the relaxation is estimated to be approximately  $\pm 0.1$  eV, which has little influence in the present discussion. The reason why the above change is very small is that the antibonding states between Cu  $3d(d\varepsilon)$  and S  $3p$  orbitals are located near at the top of the valence band [12,13], causing a large delocalization of the impurity states, except in transition metals, to form shallow impurity levels in the band gap [13].

## 3. Results and discussion

First, we show the crystal structure of  $\text{CuInS}_2:2\text{V}_{\text{Cu}}$  in Fig. 1. We determined it under the

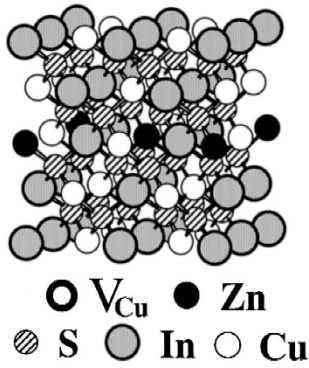


Fig. 1. Crystal structure of CuInS<sub>2</sub> doped with 2V<sub>Cu</sub>.

condition that the total energy is minimized from all atomic configurations. Next, we show the total density of states (DOS) of undoped CuInS<sub>2</sub> in Fig. 2(a) as the reference standard and the total DOS of CuInS<sub>2</sub> crystals doped with V<sub>Cu</sub>, 2V<sub>Cu</sub>, (Na<sub>Cu</sub> and

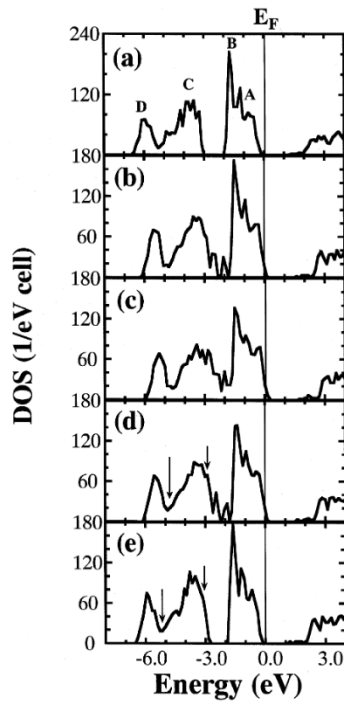


Fig. 2. (a) Total density of states (DOS) of undoped CuInS<sub>2</sub> and total DOS of CuInS<sub>2</sub> doped with (b) V<sub>Cu</sub>, (c) 2V<sub>Cu</sub>, (d) Na<sub>Cu</sub>V<sub>Cu</sub> and (e) 2Na<sub>Cu</sub>. Arrows in (d) and (e) indicate the bonding states between Na *s* or *p* states and *p* states of S close to the Na atoms.

V<sub>Cu</sub>) or 2Na<sub>Cu</sub> in Fig. 2(b)–(e), respectively. Energy is measured relative to the Fermi level ( $E_F$ ).

In Fig. 2(a), A, B, C and D refer to Cu 3*d* (*dε*)–S 3*p* antibonding states with a high Cu 3*d* (*dε*) contribution, Cu 3*d* nonbonding states (*dγ*), Cu 3*d* (*dε*)–S 3*p* bonding states with a high S 3*p* contribution, and In 5*s*–S 3*p* bonding states (the Cu 3*d* bands also have a small but finite intensity in this region), respectively. S 3*s* states are omitted in Fig. 2(a). Further details are given elsewhere [12].

For both CuInS<sub>2</sub>:V<sub>Cu</sub> in Fig. 2(b) and CuInS<sub>2</sub>:2V<sub>Cu</sub> in Fig. 2(c), we find: (1) the generation of a hole for CuInS<sub>2</sub>:V<sub>Cu</sub> and two holes for CuInS<sub>2</sub>:2V<sub>Cu</sub> at the top of the valence band; (2) a sharp DOS peak at –2.0 eV (see Fig. 2(b) and (c)) in the energy region between B and C due to dangling chemical bonds of the Cu 3*d* (*dε*)–S 3*p* orbitals; and (3) a shift in the energy levels of S 3*p* orbitals towards higher energy regions due to an increase in the Madelung energy, as discussed below. Fig. 2(d) and (e) shows that there decreases the above sharp DOS peak as there increases the concentration of Na incorporation into *p*-type CuInS<sub>2</sub> crystals. For intrinsic CuInS<sub>2</sub>:2Na<sub>Cu</sub> in Fig. 2(e), we find (1) no sharp DOS peak due to the above dangling bonds and (2) the formation of Na–S chemical bonds; strong interactions occur between Na *p* states and S *p* states located at –3.1 eV in the energy region C and between Na *s* states and S *p* states located from –5.3 eV to –5.0 eV, as shown by the arrows in Fig. 2(e). The results show good agreement with those of our previous work [10]. We summarized the calculated Madelung energies of three *p*-type doped CuInS<sub>2</sub> and intrinsic CuInS<sub>2</sub>:2Na<sub>Cu</sub> crystals under investigation in Table 1. From it, we find that while the formation of Cu vacancies increases the Madelung energy, Na incorporation in *p*-type Cu-poor CuInS<sub>2</sub> decreases it. This finding is due to charge transfer from Na 2*s* to 3*s* and 3*p* orbitals of the S atoms close to Na, resulting

Table 1

The calculated difference in the Madelung energies for between undoped and doped CuInS<sub>2</sub> crystals (eV)

V <sub>Cu</sub>	2V <sub>Cu</sub>	Na <sub>Cu</sub> V <sub>Cu</sub>	2Na <sub>Cu</sub>
+5.82	+11.22	+2.81	–9.82

in a considerable shift in the energy levels of the S  $3p$  orbitals towards lower energy regions. Thus, we conclude that the incorporation of Na, a Cu-substituting species, into  $p$ -type  $\text{CuInS}_2:\text{V}_{\text{Cu}}$  plays an important role in decreasing the concentration of donor states,  $\text{V}_{\text{S}}$ , resulting in the improved crystallinity of the  $p$ -type Cu-poor  $\text{CuInS}_2$  compared to Na-free  $\text{CuInS}_2$  films.

Next, we also investigate the stability of Na at Cu sites in  $\text{CuInS}_2$ . We carried out calculations of the electronic structure of supercells for two cases;  $\text{CuInS}_2:(\text{Na}_i \text{ and } \text{V}_{\text{Cu}})$  and  $\text{CuInS}_2:(\text{Na}_i \text{ and } [\text{Cu}]/[\text{In}] = 1)$ . In Fig. 3, for  $\text{CuInS}_2:(\text{Na}_i \text{ and } \text{V}_{\text{Cu}})$ , we show the cluster structures, including Na and its first- and second-neighbor atoms in two supercells, which have different atomic configurations each other. For  $\text{CuInS}_2:\text{Na}_i$ , we replaced one  $\text{V}_{\text{Cu}}$  site by a Cu atom in the above two clusters. The distance between the interstitial Na site in Fig. 3(a) and that in Fig. 3(b) is 2.40 Å.

For  $\text{CuInS}_2:(\text{Na}_i \text{ and } \text{V}_{\text{Cu}})$ , we find that increases in the total energy for cases I and II, as compared with that for  $\text{CuInS}_2:\text{Na}_{\text{Cu}}$  having the same numbers of atoms in the supercell, are +10.7 eV and +12.2 eV, respectively. These results indicate that  $\text{Na}_{\text{Cu}}$  is

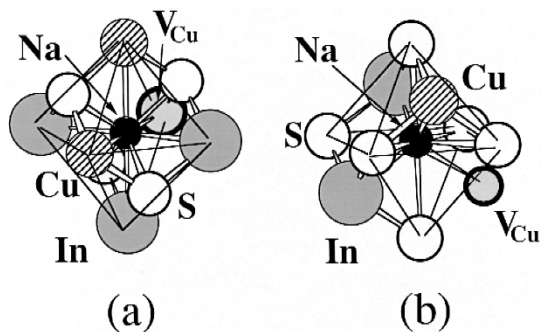


Fig. 3. Cluster structures for the two cases of  $\text{CuInS}_2$  with interstitial Na (solid circles) and Cu vacancies (hatched circles). For case I (a), the interstitial Na is surrounded by four S atoms disposed towards the corners of a tetrahedron as the first neighbors, and by two Cu atoms, three In atoms and a  $\text{V}_{\text{Cu}}$  disposed towards the corners of an octahedron as the second neighbors. For case II (b), the interstitial Na is surrounded by one Cu atom, two In atoms and a  $\text{V}_{\text{Cu}}$  disposed towards the corners of a tetrahedron as the first neighbors, and by six S atoms disposed towards the corners of an octahedron as the second neighbors. The figures of (a) and (b) are after Fig. 2 of Ref. [9].

very stable once the doped Na species occupy Cu vacancies. Moreover, we find the difference in total energy between cases I and II to be 1.5 eV, which is almost equal to the energy given by the recombination between an electron and a hole considering the band-gap energy of 1.5 eV for  $\text{CuInS}_2$ . Thus, Na moves very easily between the two structures of  $p$ -type Cu-poor  $\text{CuInS}_2:\text{V}_{\text{Cu}}$ . On the other hand, for  $\text{CuInS}_2:(\text{Na}_i \text{ and } [\text{Cu}]/[\text{In}] = 1)$ , we find that the energy difference discussed above is 2.2 eV, which is larger than the band gap value of 1.5 eV. This means that  $\text{Na}_i$  cannot move easily within stoichiometric  $\text{CuInS}_2$  crystals. These findings show that for  $p$ -type Cu-poor ( $[\text{Cu}]/[\text{In}] < 1$ )  $\text{CuInS}_2:\text{V}_{\text{Cu}}$ , interstitial Na species, except for  $\text{Na}_{\text{Cu}}$ , are very unstable and move easily toward the Cu-vacancy sites near the surface, where the material becomes more Cu-poor.

Some of the incorporated Na in  $p$ -type Cu-poor  $\text{CuInS}_2$  films was found to have segregated as Na–In–S compounds at the surface [1,2,10]. In such a case, mobile Na species play both good and bad roles on the crystallinity of  $\text{CuInS}_2$  films considering that  $\text{In}_{\text{Cu}}$  and  $\text{V}_{\text{S}}$  exhibit donor states. The formation of the anti-site defect,  $\text{In}_{\text{Cu}}$ , causes the generation of two Cu vacancies in the vicinity of the site of the  $\text{In}_{\text{Cu}}$  to keep local neutrality of electric charges. Considering the weak Cu–S bonds [13], there increases the concentration of  $\text{V}_{\text{S}}$  as there increases the concentration of the  $\text{V}_{\text{Cu}}$ , causing bad crystallinity. Thus, the Na plays a good role to reduce excess In species. Very recently, Watanabe [18] found strong correlation between the locations of Na and O near the surface of Na-incorporated  $\text{CuInS}_2$  thin films from the analysis of the experimental data using Electron Probe Micro Analysis (EPMA). Total energy calculations from all atomic configurations in the model supercells of  $\text{CuInS}_2:(\text{Na},\text{O})$  show that the formation of  $\text{Na}_{\text{Cu}}-\text{O}_{\text{S}}$  complexes, which occupy the nearest-neighbor sites is energetically favorable. While the incorporated oxygen species at S sites causes no change in the conduction type [19], they not only decrease the concentration of intrinsic defects of donors,  $\text{V}_{\text{S}}$ , but also prevent the bad crystallinity due to the generation of the  $\text{V}_{\text{S}}$ . Both the reduction of excess In species and the occupancy of the oxygen at the S-vacancy sites due to the incorporation of Na species into  $\text{CuInS}_2$  thin films explains

very well the experimental data concerning a remarkable increase in the lateral conductivity near the surface of Na-incorporated CuInS<sub>2</sub> films [11].

#### 4. Conclusions

The following conclusions were derived from the results and discussion: (1) The Na incorporation yielded a surface layer expressed as (Na,Cu)InS<sub>2</sub>; and (2) the Cu substitutions, mobile Na species and the Na<sub>Cu</sub>-O<sub>S</sub> complexes near the surface lead to an increase in the net hole concentration due to a decrease in the concentration of donor (i.e., V<sub>S</sub>, In<sub>Cu</sub> and In<sub>i</sub>) states.

#### Acknowledgements

The authors thank Mr. Watanabe of Asahi Chemical Industry for useful discussions. Thanks are also due to Professor Hiroshi Katayama-Yoshida of Osaka University who provided support and encouragement during the course of this study. One of the authors (T.Y.) thanks Dr. Jürgen Sticht of Molecular Simulations

#### References

- [1] T. Watanabe, H. Nakazawa, M. Matsui, H. Ohbo, T. Nakada, *Sol. Energy Mater. Sol. Cells* 49 (1997) 357.
- [2] T. Watanabe, H. Nakazawa, M. Matsui, H. Ohbo, T. Nakada, Technical Digest of the 9th Int. Photovoltaic Science and Engineering Conf., Miyazaki (1996) 257, (Int. PVSEC-9 Office, Tokyo, 1996).
- [3] L. Stolt, Technical Digest of the 9th Int. Photovoltaic Science and Engineering Conf., Miyazaki (1996) 135, (Int. PVSEC-9 Office, Tokyo, 1996).
- [4] T. Nakada, H. Ohbo, M. Fukuda, A. Kunioka, *Sol. Energy Mater. Sol. Cells* 49 (1997) 261.
- [5] T. Nakada, H. Ohbo, M. Fukuda, A. Kunioka, Technical Digest of the 9th Int. Photovoltaic Science and Engineering Conf., Miyazaki (1996) 139, (Int. PVSEC-9 Office, Tokyo, 1996).
- [6] T. Nakada, D. Iga, H. Ohbo, A. Kunioka, *Jpn. J. Appl. Phys.* 36 (1997) 732.
- [7] Y. Ogawa, A.J. Waldau, T.H. Hua, Y. Hashimoto, K. Ito, *Appl. Surf. Sci.* 92 (1996) 232.
- [8] R. Scheer, M. Alt, I. Luck, H.J. Lewerentz, *Sol. Energy Mater. Sol. Cells* 49 (1997) 423.
- [9] T. Yamamoto, *Jpn. J. Appl. Phys.* 37 (1998) L1478.
- [10] K. Fukuzaki, S. Kohiki, H. Yoshikawa, S. Fukushima, T. Watanabe, I. Kojima, *Appl. Phys. Lett.* 73 (1998) 1385.
- [11] T. Watanabe, H. Nakazawa, M. Matsui, *Jpn. J. Appl. Phys.* 37 (1998) L1370.
- [12] T. Yamamoto, H. Katayama-Yoshida, *Jpn. J. Appl. Phys.* 34 (1995) L1584.
- [13] T. Yamamoto, H. Katayama-Yoshida, *Inst. Phys. Conf. Ser.* 152 (1998) 37.
- [14] W. Kohn, L.J. Sham, *Phys. Rev.* 140 (1965) A1133.
- [15] L. Hedin, B.I. Lundquist, *J. Phys. C4* (1971) 3107.
- [16] U. von Barth, L. Hedin, *J. Phys. C5* (1972) 1629.
- [17] A.R. Williams, J. Kuebler, C.D. Gelatt, *Phys. Rev. B* 19 (1979) 6094.
- [18] T. Watanabe, private communications.
- [19] T. Yamamoto, H. Katayama-Yoshida, *Jpn. J. Appl. Phys.* 35 (1996) L370.